Pharmaceutical Research, Vol. 22, No. 8, August 2005 (© 2005)
DOI: 10.1007/s11095-005-5262-z

Research Paper

A Quantitative Assessment of the Significance of Molecular Mobility as a Determinant for the Stability of Lyophilized Insulin Formulations

Sumie Yoshioka[1,2] and Yukio Aso[1]

Received October 24, 2004; accepted March 15, 2005

Purpose. The purpose was to explore a method for quantitatively assessing the contribution of molecular mobility to the chemical reactivity of amorphous solids. Degradation of insulin in lyophilized formulations containing trehalose and poly(vinylpyrrolidone)(PVP) was chosen as a model system, and the temperature- and glass transition temperature (T_g)-dependence of the degradation rate was analyzed to obtain the relative contributions of molecular mobility and that of the chemical activational barrier reflected in the energy of activation.

Methods. Insulin degradation and dimerization in lyophilized trehalose and PVP formulations were monitored at various relative humidities (6–60% RH) and temperatures (10–60°C) by reverse-phase high-performance liquid chromatography (HPLC) and high-performance size-exclusion chromatography (HP-SEC), respectively. The T_g and fragility parameter of the lyophilized insulin formulations were determined by differential scanning calorimetry (DSC).

Results. Insulin degradation in the initial stage was describable with first-order kinetics for both of the trehalose and PVP formulations. The temperature- and T_g-dependence of the degradation rate indicated that the reactivity of insulin in the trehalose formulation is affected by molecular mobility at low humidity (12% RH), such that the ratio of the observed rate constant (k') to the rate constant governed only by the activational barrier (k) was 0.051 at the T_g. At higher humidities, in contrast, the value of k'/k was much higher (0.914, 0.978, and 0.994 for 23% RH, 33% RH, and 43% RH, respectively), indicating that insulin degradation rate is determined predominantly by the activational barrier. For insulin degradation in the PVP formulation at temperatures below T_g, the contribution of molecular mobility to the degradation rate appeared to be negligible, as the extrapolated value of t_{90} at the T_g exhibited a large difference between the formulations with differing T_g values (because of differing water contents).

Conclusions. The reactivity of insulin in the trehalose and PVP formulations can be described by an equation including factors reflecting the activational barrier (activation energy and frequency coefficient) and factors reflecting the molecular mobility (T_g, fragility parameter and a constant representing the relationship between the molecular mobility and the reaction rate). Thus, analysis of temperature dependence based on the proposed equation allows quantitative assessment of the significance of molecular mobility as a factor affecting chemical reactivity.

KEY WORDS: Adam-Gibbs-Vogel equation; glass transition temperature, insulin, lyophilized formulation; molecular mobility.

INTRODUCTION

Recent studies have demonstrated that molecular mobility is an important factor that affects the chemical (1–7) and physical (8–12) stability of amorphous pharmaceuticals including drugs of small molecular weight, peptides, and proteins (13–20). The contribution of molecular mobility to the rates of chemical degradations or physical changes such as crystallization is difficult to evaluate quantitatively, however, because thermodynamic factors also affect these rates. The chemical reactivity of amorphous solids is affected by molecular mobility as well as the chemical activational barrier, reflected in the energy of activation for the reaction. The contribution of molecular mobility to the reactivity has not been quantitatively evaluated in comparison with that of the activational barrier, however.

In formulation development and stability evaluation for amorphous pharmaceuticals, it is very important to assess the contribution of molecular mobility to the chemical reactivity. If the molecular mobility is found to be the predominant determinant of the reactivity, the chemical stability may be improved by increasing the glass transition temperature (T_g) using excipients with high T_g. If the contribution of molecular mobility to the reactivity is negligible, stability prediction by extrapolating stability data obtained under accelerated con-

[1] National Institute of Health Sciences, Setagaya-ku, Tokyo 158-8501, Japan.
[2] To whom correspondence should be addressed. (e-mail: yoshioka@nihs.go.jp)

ABBREVIATIONS: DSC, differential scanning calorimetry; HPLC, high-performance liquid chromatography; HP-SEC, high-performance size-exclusion chromatography; PVP, poly(vinylpyrrolidone); RH, relative humidity; RP-HPLC, reverse-phase HPLC.

ditions may be possible even if the extrapolation extends across the T_g.

In this study, we explored a method for quantitatively assessing the significance of molecular mobility as a factor affecting chemical reactivity. Degradation of insulin in lyophilized formulations containing either trehalose or poly (vinylpyrrolidone)(PVP) was chosen as a model system, and the temperature- and T_g-dependence of the degradation rate was analyzed to obtain the relative contributions of molecular mobility and that of the activational barrier. It is well known that the major degradation pathways of insulin in solution and in the solid state are deamidation and dimerization via a cyclic imide intermediate (14,21–23).

MATERIALS AND METHODS

Preparation of Lyophilized Insulin Formulation

Human zinc insulin (Humulin® RU-100) was purchased from Eli Lilly & Co, and converted into the zinc-free neutral form by dialysis as reported (24). Trehalose (203-02252) or PVP (K-30, Wako Pure Chemical Ind. Ltd., Osaka) was dissolved in the zinc-free insulin solution to make a 5 mg/ml solution, and the pH was adjusted to 4.0. The resulting solution contained insulin and trehalose or PVP (1:1.5 w/w). Four hundred microliters of the solution were frozen in a polypropylene sample tube (10 mm diameter), and then dried at a vacuum level below 5 Pa for 23.5 h in a lyophilizer (Freezevac C-1, Tozai Tsusho Co., Tokyo). The shelf temperature was between −35 and −30°C for the first 1 h, 20°C for the subsequent 19 h, and 30°C for the last 3.5 h.

Lyophilized samples with various water contents were obtained by storage at 15°C for 24 h in a desiccator with a saturated solution of $LiBr \cdot H_2O$ [6% relative humidity (RH)], $LiCl \cdot H_2O$ (12% RH), potassium acetate (23% RH), $MgCl_2 \cdot 6H_2O$ (33% RH), $K_2CO_3 \cdot 2H_2O$ (43% RH) or $NaBr \cdot 2H_2O$ (60% RH).

Determination of T_g and Fragility Parameter by Differential Scanning Calorimetry (DSC)

Lyophilized samples with various water contents were placed in a hermetic pan, and thermograms were obtained in the temperature range from 40°C lower than the T_g to 40°C higher than the T_g at a heating scan rate of 5°C/min (2920; TA Instruments, DE). Temperature calibration was performed using indium. The measured T_g values are shown in Table I. The fragility parameter (m) for the trehalose formulation was calculated from the glass transition width determined from the extrapolated onset and offset (25,26). The calculated m value was 45 and 50 at 12% RH and 43% RH, respectively.

Table I. The T_g of lyophilized insulin formulations determined by DSC

	T_g (°C)	
Relative humidity (% RH)	Trehalose	PVP
6	—	160
12	44	129
23	26	103
33	10	85
43	0.8	80
60	—	56

—, Not determined.

Determination of Insulin Degradation and Dimerization Rates

Lyophilized samples containing various amounts of water were stored in tightly screw-capped tubes at a constant temperature (10–60°C), removed at various times, and stored in liquid nitrogen until assayed. Samples were dissolved in 1.5 ml of 0.01 M $(NH_4)_2SO_4$ (pH 2.2, adjusted with concentrated H_2SO_4) and subjected to reverse-phase high-performance liquid chromatography (RP-HPLC) and high-performance size-exclusion chromatography (HP-SEC).

The concentration of intact insulin was quantified using a modular RP-HPLC consisting of two Shimadzu pumps with a mixer (LC-10AD), an injector (SIL-10ADVP), and a UV detector (SPD-10A), as reported (27). The column used was Inertsil WP-300 (C8, 4.6 mm × 250 mm, GL Science Inc.) maintained at 35°C. Elutions were performed using a mixture of 0.01 M $(NH_4)_2SO_4$ (pH 2.2, adjusted with concentrated H_2SO_4) and acetonitrile solution of 0.07% (v/v) trifluoroacetic acid (72.5:27.5) for 1 min. The ratio of the acetonitrile solution increased linearly from 27.5% to 30% in 15 min and 30% to 35% in 22 min. The detection wavelength was 214 nm.

Higher molecular weight transformation was determined by HP-SEC, using a Hitachi UV detector (L-4000) and a column (Protein-Pak 125, 7.8 mm × 300 mm, Waters) maintained at 25°C, as reported (21). A 2.5 M acetic acid solution containing 4 mM L-arginine and 4% (v/v) acetonitrile was eluted at a rate of 1 ml/min. The amount of insulin within an intact molecule of a given size was measured based on the peak height.

RESULTS AND DISCUSSION

Figure 1 shows the time courses of insulin degradation at 43% RH in the PVP formulation determined by RP-HPLC. Similar time courses were also obtained at 6% RH, 12% RH, 23% RH, 33% RH, and 60% RH in the PVP formulation, and at 12% RH, 23% RH, 33% RH, and 43% RH in the trehalose formulation. The major degradation pathway is known to be deamidation through a cyclic imide intermediate (14,21–23). Degradation in the initial stage was describable with first-order kinetics for both of the trehalose and PVP formulations. The time required for 10% degradation (t_{90}) was calculated from the apparent first-order rate constant. Time courses of insulin dimerization determined by HP-SEC were also describable with first-order kinetics in the initial stage (data are not shown).

Figure 2 shows the temperature dependence of the calculated t_{90} for insulin degradation and dimerization. For

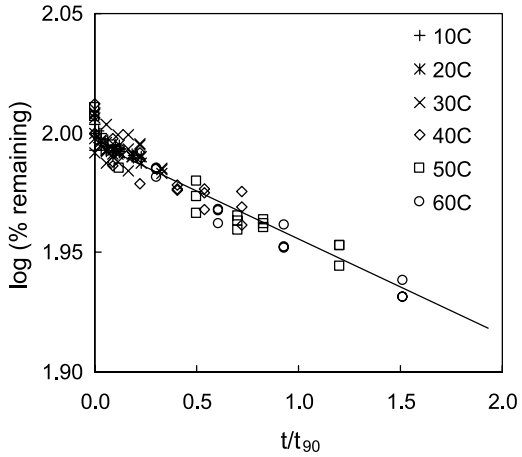

Fig. 1. Time courses of insulin degradation in PVP formulation at 43% RH at various temperatures. Time is scaled to the t_{90} for each temperature.

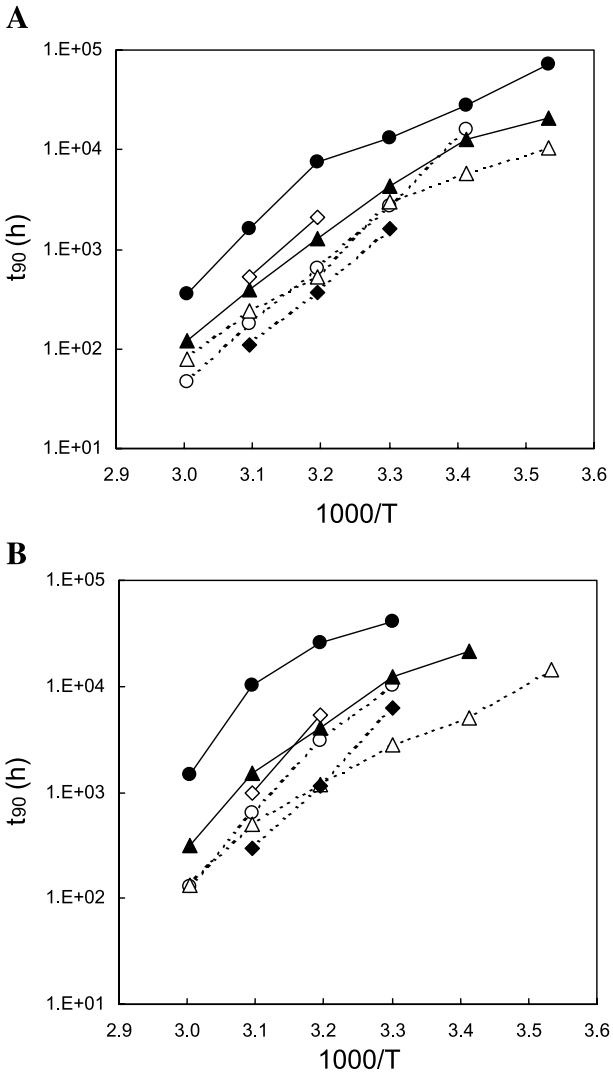

Fig. 2. Temperature dependence of t_{90} for insulin degradation (A) and dimerization (B). (●) trehalose at 12% RH; (◇) trehalose 23% RH; (○) trehalose at 33% RH; (◆) trehalose 43% RH; (▲) PVP at 12% RH; (△) PVP at 43% RH.

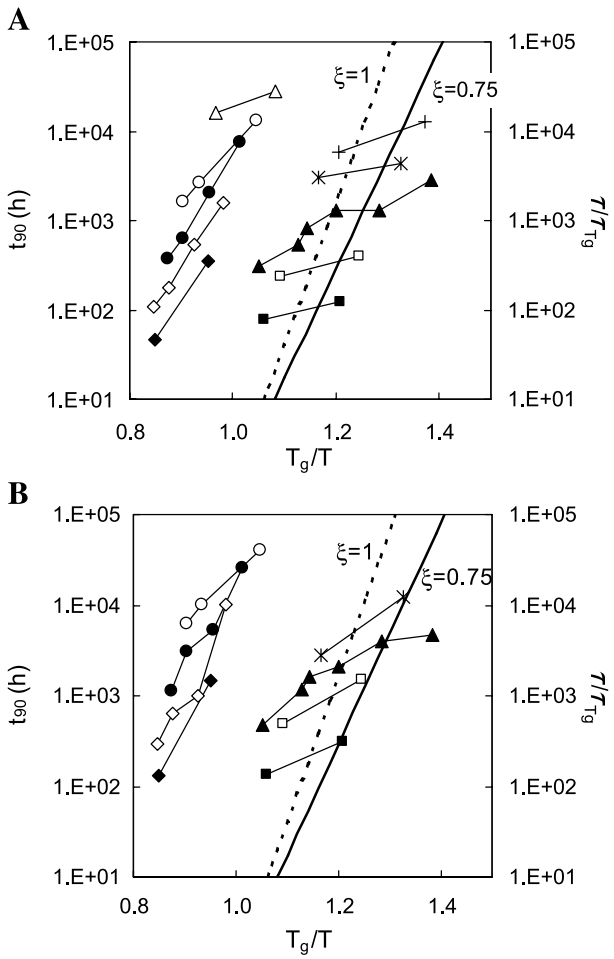

Fig. 3. T_g dependence of t_{90} determined at a constant temperature for insulin degradation (A) and dimerization (B). Trehalose at various RHs (12% RH–43% RH) at 60°C (◆), 50°C (◇), 40°C (●); 30°C (○), and 20°C (△); PVP at various RHs (6% RH–60% RH) at 60°C (■), 50°C (□), 40°C (▲), 30°C (✳), and 20°C (+). Dotted and solid bold lines represent the structural relaxation time calculated according to the AGV equation using $\xi = 1$ and 0.75, respectively.

both of the trehalose and PVP formulations, t_{90} was larger at lower humidity. Comparison of t_{90} at 12% RH indicated that the trehalose formulation was more stable than the PVP formulation. This difference in t_{90} between the trehalose and PVP formulations decreased at 43% RH.

Figure 3 shows the T_g dependence of t_{90} obtained at a constant temperature (20–60°C). For both of the trehalose and PVP formulations, t_{90} increased with increasing T_g associated with decreasing water content. The trehalose formulation exhibited a t_{90} at T_g that was approximately two orders of magnitude larger than the PVP formulation for insulin degradation and dimerization at 40°C.

Simulations of the Effect of T_g, ΔH, and α on t_{90}

For a reaction occurring in the physical state in which the rate-determining step involves molecular diffusion (e.g., in the solid state), the rate constant (k') can be related to the rate constant at the condition under which reactants have

high diffusibility (e.g., in solution) (k) according to Eq. (1), as described by Karel and Saguy (28)

$$k' = k\left(\frac{1}{1+\frac{k}{\alpha D_r}}\right) = k\left(\frac{\alpha D_r}{k+\alpha D_r}\right) \quad (1)$$

where D_r is diffusion coefficient of the reactant and α is a constant representing the correlation between D_r and reaction rate. When αD is much larger than k ($\alpha D_r \gg k$), the value in the parentheses equals to unit, conforming k' to k. As D_r decreases, the value in the parentheses decreases, making k' smaller than k. As clearly shown by Eq. (1), the constant α corresponds to the slope of the k' *vs.* D_r plot when αD is much smaller than *k* ($\alpha D_r \ll k$). The value of α may depend on the degradation mechanism, that is, whether the degradation involves translational or rotational motions of entire molecules, or intramolecular motions of specific portions of the molecule.

D_r in Eq. (1) can be estimated (4) from structural relaxation time (τ) according to Eq. (2):

$$\frac{D_{r2}}{D_{r1}} \approx \left(\frac{T_2}{T_1}\right)\left(\frac{\tau_1}{\tau_2}\right)^{\xi} \quad (2)$$

where ξ is a constant that represents the degree of decoupling between D_r and τ. τ can be calculated from T_g and fragility parameter (m) using the Vogel-Tammann-Fulcher (VTF) (29) and Adam-Gibbs-Vogel (AGV) (30) equations [Eqs. (3) and (4)] above and below the T_g, respectively.

$$\tau(T) = \tau_0 \exp\left(\frac{DT_0}{T-T_0}\right) \quad (3)$$

$$\tau(T,T_f) = \tau_0 \exp\left(\frac{DT_0}{T-(T/T_f)T_0}\right) \quad (4)$$

where τ_0 is the relaxation time at the high temperature limit (10^{-14} s), T_f is fictive temperature (approximated by T_g for newly formed glasses), $D = 2.303(m_{min})^2/(m - m_{min})$, $T_0 = T_g(1 - m_{min}/m)$, and $m_{min} = \log(\tau_{T_g}/\tau_0)$.

On the other hand, k in Eq. (1) can be related to the activation energy (ΔH) and frequency factor (A) according to Eq. (5):

$$k = A \exp\left(\frac{-\Delta H}{RT}\right) \quad (5)$$

where R is the gas constant. Therefore, Eq. (1) can be written as Eq. (6), by substituting Eq. (2) for D_r and Eq. (5) for k. k' in Eq. (6) can be converted to t_{90} (the time required for 10% degradation), which is convenient for comparing with relaxation time. Thus, the dependence of t_{90} on factors reflecting the activational barrier (ΔH and A) and factors reflecting the molecular mobility (T_g, m, and α) can be described by Eq. (6), which allows quantitative assessment of the significance of molecular mobility as a determinant of t_{90}.

$$k' = \frac{A \exp\left(\frac{-\Delta H}{RT}\right)\alpha T\left(\frac{1}{\tau}\right)^{\xi}}{A \exp\left(\frac{-\Delta H}{RT}\right) + \alpha T\left(\frac{1}{\tau}\right)^{\xi}} = \frac{-\ln(0.9)}{t_{90}} \quad (6)$$

To assess the effects of T_g, ΔH, and α on the temperature dependence of t_{90}, simulations based on Eq. (6), using representative values for various parameters, were carried out. The results are shown in Fig. 4, where A and m were assumed to be 10^{14} s^{-1} and 70, respectively. Figure 4A shows the temperature dependence of t_{90} calculated using Eq. (6) as a function of T_g, assuming that ΔH is equal to 30 kcal/mol and α is 10^{-8}. Differences in water content change the T_g, and as

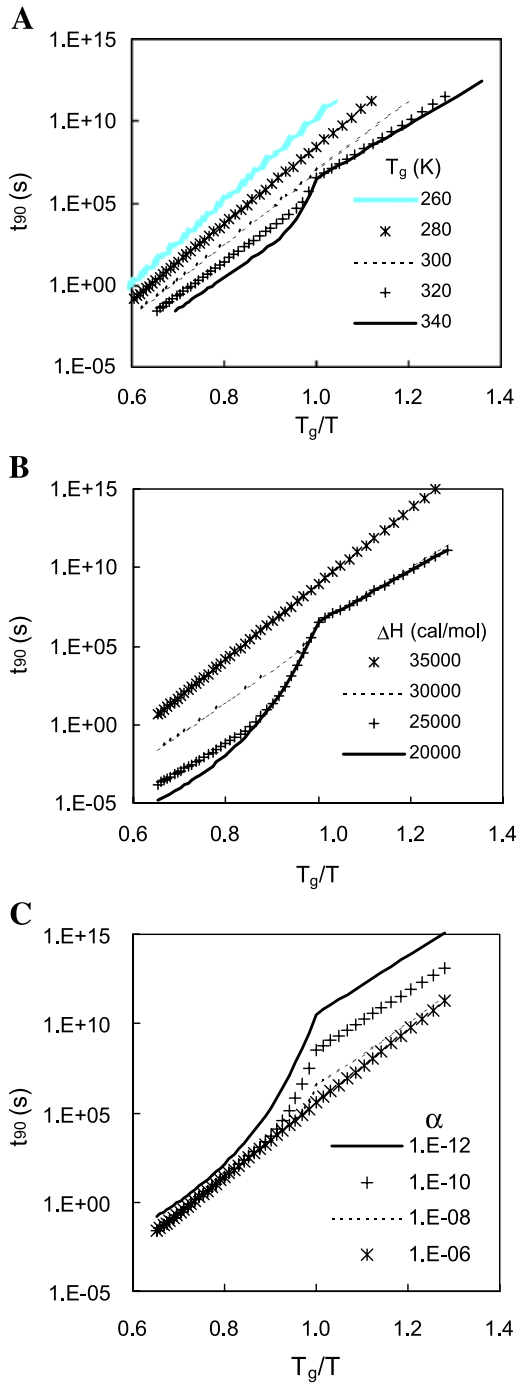

Fig. 4. Effect of T_g, ΔH, and α on the temperature dependence of t_{90} calculated according to Eq. (6) (m = 70). (A) t_{90} as a function of T_g (K) when ΔH = 30 kcal/mol and $\alpha = 10^{-8}$. (B) t_{90} as a function of ΔH when T_g = 320 K and $\alpha = 10^{-8}$. (C) t_{90} as a function of α when T_g = 320 K and ΔH = 30 kcal/mol.

a consequence bring about changes in the shape of temperature dependence for t_{90}, as shown in Fig. 4A, in which ΔH and α are assumed to be not affected by differing water contents. As T_g decreases (molecular mobility increases), the contribution of αD_r to k' in Eq. (1) decreases because of a larger value of αD_r compared to k. Thus, k' is determined by k to a larger extent, resulting in a smaller change in the slope of the temperature dependence occurring around T_g.

Figure 4B shows the temperature dependence of t_{90} as a function of ΔH, assuming that T_g is equal to 320 K, and α is 10^{-8}. As ΔH increases, the contribution of αD_r to k' decreases because of a smaller value of k compared to αD_r, resulting in a smaller change in the slope of the temperature dependence occurring around T_g.

Figure 4C shows the temperature dependence of t_{90} as a function of α, assuming that T_g equals 320 K, and ΔH is 30 kcal/mol. As α increases, the contribution of αD_r to k' decreases, resulting in a smaller change in the slope of temperature dependence occurring around T_g.

As shown in Fig. 4A, increases in T_g increase the contribution of molecular mobility to k'. To compare the contribution of molecular mobility with that of the activational barrier, k'/k was calculated for the model reaction shown in Fig. 4A, and the results are shown in Fig. 5. When T_g is low (280 K), the contribution of the activational barrier is predominant regardless of temperature. In contrast, when T_g is high (340, 320, or 300 K), the contribution of the activational barrier is predominant at lower T_g/T (higher temperature), and it decreases substantially with decreasing temperature (approaching T_g). This is because the slope of temperature dependence for the τ calculated by the VTF equation is larger than ΔH (30 kcal/mol) at temperatures near the T_g. When temperature decreases below the T_g, the slope of the k'/k *vs.* T_g/T curve becomes positive, because ΔH is larger than the slope of temperature dependence for the τ calculated by the AGV equation. Equation (6) can be applied only for reactions that exhibit an activation energy independent of temperature.

Significance of Molecular Mobility as a Determinant of t_{90} for Insulin Degradation and Dimerization

Figure 6 shows the $t_{90} - T_g/T$ plots for insulin degradation and dimerization in trehalose and PVP formulations

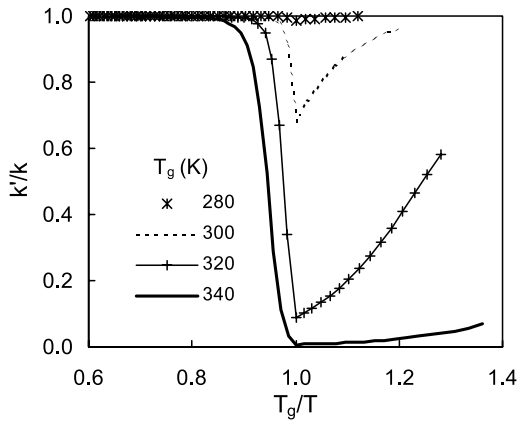

Fig. 5. Contribution of activational barrier to the t_{90} shown in Fig. 4A.

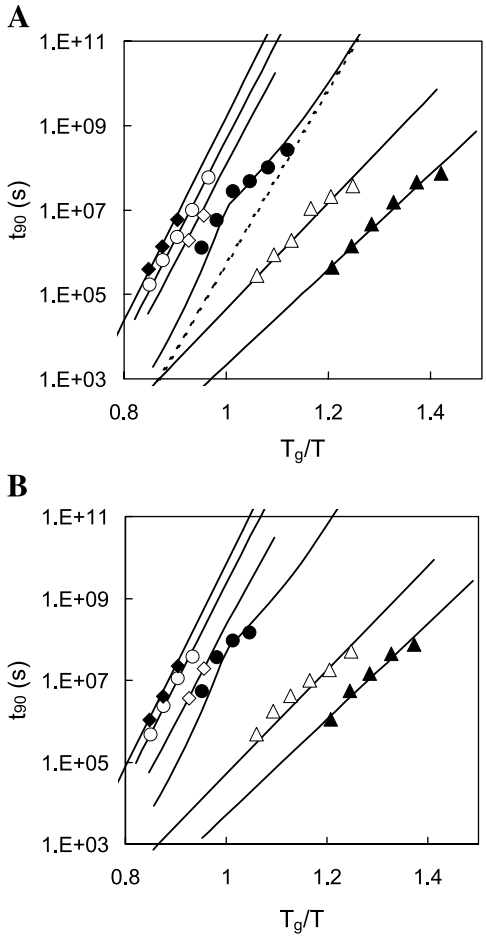

Fig. 6. Temperature dependence of t_{90} for insulin degradation (A) and dimerization (B). (●) trehalose 12% RH; (◇) trehalose 23% RH; (○) trehalose 33% RH; (◆) trehalose 43% RH; (▲) PVP 12% RH; (△) PVP 43% RH. Solid line for the t_{90} observed at 12% RH in insulin–trehalose formulation represents the least-squared regression curve according to Eq. (6), and dotted line represents the t_{90} calculated from k. Lines for other conditions represent the least-squared regression curve according to Eq. (5).

with differing T_g values attributable to differing water contents. Comparison of the $t_{90} - T_g/T$ plots for insulin degradation (Fig. 6A) with the simulated plots shown in Fig. 4A indicates that t_{90} for insulin degradation at 12% RH in the trehalose formulation is affected by the molecular mobility of the matrix. Curve-fitting of the observed t_{90} to Eq. (6), assuming τ_0 of 10^{-14} s, A of 10^{14} s^{-1}, m of 45 (calculated from the width of the glass transition measured by DSC) and ξ of 0.75, provided a ΔH estimate of 30.0 kcal/mol and an α estimate of 1×10^{-9}. The ξ value of 0.75, which is considered to be the lower limit of ξ representing the degree of decoupling between τ and D_r (31), gave a best fit. The dotted line in Fig. 6A represents the temperature dependence of t_{90} calculated from k, namely t_{90} determined by the activational barrier. The value of k'/k was calculated to be 0.051 at the T_g, indicating that the reaction rate is determined predominantly by the molecular mobility of the matrix. Thus, the observed t_{90} for insulin degradation at 12% RH appears to correspond to the simulated case with a high T_g value shown in Figs. 4A and 5.

For the trehalose formulations with lower T_g values, a linear temperature dependence was observed at temperatures above T_g, giving a ΔH estimate of 31.5, 30.8, and 30.4 kcal/mol for 23% RH, 33% RH, and 43% RH, respectively. The values of k'/k at T_g, calculated from the ΔH estimate and the t_{90} value at T_g obtained by extrapolation of the observed values, were 0.914, 0.978, and 0.994 for 23% RH, 33% RH, and 43% RH, respectively. These findings suggest that the reaction rate is determined predominantly by the activational barrier, and molecular mobility is sufficiently high such that molecular mobility is not involved in the rate-determining step. Thus, the t_{90} for insulin degradation under these conditions appears to correspond to the simulated case with a low T_g value shown in Figs. 4A and 5.

The t_{90} for insulin degradation in the trehalose formulations observed at temperatures above T_g was normalized against the t_{90} at T_g, and plotted against T_g/T in Fig. 7 in comparison with the structural relaxation time (τ) calculated according to the VTF equation from the values of T_g and m measured by DSC. This normalized $t_{90} - T_g/T$ plot exhibited a linear relationship with a smaller slope than the τ calculated using a ξ value of 0.75. This finding supports the thought that the contribution of molecular mobility to the reaction rate is negligible under these conditions.

For insulin degradation in the trehalose formulation, it may be concluded that differences in water content do not bring about significant differences in ΔH, but rather differences in the contribution of molecular mobility to the degradation rate.

For insulin degradation in the PVP formulation, it cannot be judged whether the slope of the $t_{90} - T_g/T$ plot changes around the T_g, because of the lack of data at temperatures above T_g (Fig. 6A). The slope below T_g was close to that observed for the trehalose formulation with the highest T_g value, and smaller than those observed in the trehalose formulations with lower T_g values, the t_{90} of which is determined predominantly by the activational barrier. However, the value of t_{90} at T_g (extrapolated from observed values) exhibited a large difference between the PVP formulations with differing T_g values because of differing water contents, indicating that the molecular mobility of the matrix is not involved in the rate-determining step. Insulin degradation under these conditions appears to correspond to the simulated case in which t_{90} is determined by the activational barrier shown in Fig. 4A. Curve fitting to Eq. (6) provided estimates of A of 10^7 s^{-1} as well as ΔH of 20.8 and 20.4 kcal/mol for 12% RH and 42% RH, respectively.

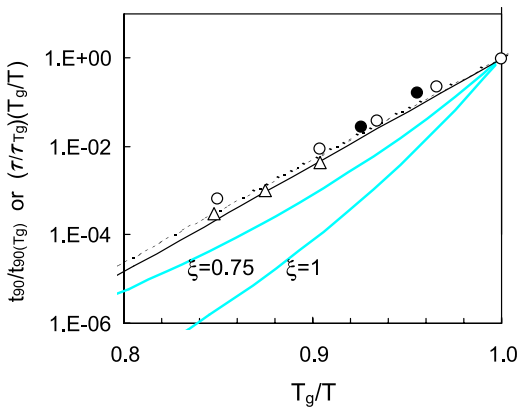

Fig. 7. Temperature dependence of the normalized t_{90} for insulin degradation in the trehalose formulation obtained above T_g [(●) 23%RH, (○) 33% RH, (△) 43% RH] fitted to the Arrhenius equation (dotted and solid lines represent regression curves for t_{90} at 23% RH and 43% RH, respectively, calculated using each ΔH estimate and a common A value of 10^{14} s^{-1}). t_{90} is compared to the structural relaxation time calculated according to the VTF equation using an m value of 50 and ξ values of 1 and 0.75 (——).

The T_g dependence of t_{90} for the PVP formulation is compared with the structural relaxation time calculated according to the AGV equation using a ξ value of 0.75 in Fig. 3. The slope of the $t_{90} - T_g/T$ plot for the data obtained at a constant temperature but at different humidities was much smaller than that for the structural relaxation time, supporting the thought that the contribution of molecular mobility to the degradation rate is negligible. However, the slope of the $t_{90} - T_g/T$ plot should be zero without the effect of molecular mobility, if A and ΔH are independent of humidity (water content). The observed positive slope suggests that a difference in water content brings about a small difference in ΔH. This idea is supported by the ΔH values obtained by curve-fitting (Fig. 6A), which tended to increase slightly with decreasing water content.

Insulin dimerization in the trehalose and PVP formulations exhibited temperature dependence similar to that of insulin degradation, as shown in Fig. 6B. The contribution of molecular mobility to the t_{90} appeared to be small, except for the t_{90} observed at 12% RH in the trehalose formulation. Curve-fitting to Eq. (6) gave slightly greater values of ΔH compared with those for insulin degradation both for the trehalose (31.8, 31.5, and 31.1 kcal/mol for 23% RH, 33% RH, and 43% RH, respectively) and PVP formulations (21.5 and 20.5 kcal/mol for 12% RH and 43% RH).

Significant differences were observed in insulin degradation and dimerization behaviors between the trehalose and PVP formulations. The reactivity of insulin in the trehalose formulation was much smaller than that in the PVP formulation, when compared at the same T_g/T (namely same molecular mobility of the matrix), as shown in Fig. 3. A and ΔH were estimated to be 10^{14} s^{-1} and approximately 30 kcal/mol, respectively, for the trehalose formulation, compared with 10^7 s^{-1} and approximately 20 kcal/mol for the PVP formulation. These findings suggest that reaction mechanisms are different between the two formulations. The much smaller value of A obtained for the PVP formulation may indicate a reaction mechanism other than a simple monomolecular reaction. One other possible explanation for these differences may be qualitative and quantitative differences in insulin-excipient interaction behavior or in phase separation behavior. In addition, PVP may react with insulin to produce a PVP–insulin adduct in a similar manner as was observed for a PVP–hexapeptide adduct (32). Further studies are required to interpret the differences in the reactivity between the trehalose and PVP formulations. In addition, the relationship between the matrix mobility described in the present article and the local mobility of reactants such as polymer side chains and water molecules needs to be elucidated in order to discuss the effect of molecular mobility based on the degradation mechanism.

CONCLUSION

The reactivity of insulin in the trehalose and PVP formulations can be described by Eq. (6) including factors reflecting the activational barrier (ΔH and A) and factors reflecting the molecular mobility (T_g, m, and α). Thus, analysis of temperature dependence based on Eq. (6) allows quantitative assessment of the significance of molecular mobility as a determinant of chemical reactivity.

ACKNOWLEDGMENT

The authors would like to thank Prof. G. Zografi of the University of Wisconsin-Madison for his valuable comments and encouragement during the preparation of this manuscript.

REFERENCES

1. S. P. Duddu and K. Weller. Importance of glass transition temperature in accelerated stability testing of amorphous solids: case study using a lyophilized aspirin formulation. *J. Pharm. Sci.* **85**:345–347 (1996).
2. L. Streefland, A. D. Auffret, and F. Franks. Bond cleavage reactions in solid aqueous carbohydrate solutions. *Pharm. Res.* **15**:843–849 (1998).
3. M. C. Lai, M. J. Hageman, R. L. Schowen, R. T. Borchardt, and E. M. Topp. Chemical stability of peptides in polymers. 2. Discriminating between solvent and plasticizing effects of water on peptide deamidation in poly(vinylpyrrolidone). *J. Pharm. Sci.* **88**:1081–1089 (1999).
4. Y. Guo, S. R. Byrn, and G. Zografi. Physical characteristics and chemical degradation of amorphous quinapril hydrochloride. *J. Pharm. Sci.* **89**:128–143 (2000).
5. J. Li, Y. Guo, and G. Zografi. The solid-state stability of amorphous quinapril in the presence of β-cyclodextrins. *J. Pharm. Sci.* **91**:229–243 (2002).
6. S. Yoshioka, Y. Aso, and S. Kojima. Temperature dependence of bimolecular reactions associated with molecular mobility in lyophilized formulations. *Pharm. Res.* **17**:925–929 (2000).
7. S. Yoshioka, Y. Aso, and S. Kojima. Temperature- and glass transition temperature-dependence of bimolecular reaction rates in lyophilized formulations described by the Adam-Gibbs-Vogel equation. *J. Pharm. Sci.* **93**:1062–1069 (2004).
8. V. Andronis, M. Yoshioka, and G. Zografi. Effect of sorbed water on the crystallization of indomethacin from the amorphous state. *J. Pharm. Sci.* **86**:346–351 (1997).
9. V. Andronis and G. Zografi. Crystal nucleation and growth of indomethacin polymorphs from the amorphous state. *J. Non-Cryst. Solids* **271**:236–248 (2000).
10. Y. Aso, S. Yoshioka, and S. Kojima. Explanation of the crystallization rate of amorphous nifedipine and phenobarbital from their molecular mobility as measured by ^{13}C nuclear magnetic resonance relaxation time and the relaxation time obtained from the heating rate dependence of the glass transition temperature. *J. Pharm. Sci.* **90**:798–806 (2001).
11. D. Zhou, G. G. Z. Zhang, D. Law, D. J. W. Grant, and E. A. Schmitt. Physical stability of amorphous pharmaceuticals: importance of configurational thermodynamic quantities and molecular mobility. *J. Pharm. Sci.* **91**:1863–1872 (2002).
12. Y. Aso, S. Yoshioka, and S. Kojima. Molecular mobility-based prediction of the crystallization rate of amorphous nifedipine and phenobarbital in PVP solid dispersions of the paracetamol amorphous form. *J. Pharm. Sci.* **93**:384–391 (2004).
13. S. P. Duddu, G. Zhang, and P. R. Dal Monte. The relationship between protein aggregation and molecular mobility below the glass transition temperature of lyophilized formulations containing a monoclonal antibody. *Pharm. Res.* **14**:596–600 (1997).
14. R. G. Strickley and B. D. Anderson. Solid-state stability of human insulin II. Effect of water on reactive intermediate partitioning in lyophiles from pH 2–5 solutions: stabilization against covalent dimer formation. *J. Pharm. Sci.* **86**:645–653 (1997).
15. S. Yoshioka, Y. Aso, and S. Kojima. Dependence of the molecular mobility and protein stability of freeze-dried γ-globulin formulations on the molecular weight of dextran. *Pharm. Res.* **14**:736–741 (1997).
16. S. Yoshioka, Y. Aso, Y. Nakai, and S. Kojima. Effect of high molecular mobility of poly(vinyl alcohol) on protein stability of lyophilized γ-globulin formulations. *J. Pharm. Sci.* **87**:147–151 (1998).
17. S. D. Allison, M. C. Manning, T. R. Randolph, K. Middleton, A. Davis, and J. F. Carpenter. Optimization of storage stability of lyophilized actin using combinations of disaccharides and dextran. *J. Pharm. Sci.* **89**:199–214 (2000).
18. S. Yoshioka, Y. Aso, and S. Kojima. Usefulness of the Kohlrausch-Williams-Watts stretched exponential function to describe protein aggregation in lyophilized formulations and the temperature dependence near the glass transition temperature. *Pharm. Res.* **18**:256–260 (2001).
19. S. Yoshioka, S. Tajima, Y. Aso, and S. Kojima. Inactivation and aggregation of β-galactosidase in lyophilized formlation described by Kohlrausch-Williams-Watts stretched exponential function. *Pharm. Res.* **20**:1655–1660 (2003).
20. W. Garzon-Rodriguez, R. L. Koval, S. Chongprasert, S. Krishnan, T. W. Randolph, N. W. Warne, and J. F. Carpenter. Optimizing storage stability of lyophilized recombinant human interleukin-11 with disaccharide/hydroxyethyl starch mixtures. *J. Pharm. Sci.* **93**:684–696 (2004).
21. J. Brange, S. Havelund, and P. Hougaard. Chemical stability of insulin. 2. Formulation of higher molecular weight transformation products during storage of pharmaceutical preparations. *Pharm. Res.* **9**:727–734 (1992).
22. R. T. Darrington and B. D. Anderson. Effect of insulin concentration and self-association on the partitioning of its a-21 cyclic anhydride intermediate to desamido insulin and covalent dimer. *Pharm. Res.* **12**:1077–1084 (1995).
23. M. J. Pikal and D. R. Rigsbee. The stability of insulin in crystalline and amorphous solids: observation of greater stability for the amorphous form. *Pharm. Res.* **14**:1379–1387 (1997).
24. R. T. Darrington and B. D. Anderson. The role of intramolecular nucleophilic catalysis and the effects of self-association on the deamidation of human insulin at low pH. *Pharm. Res.* **11**:784–793 (1994).
25. C. T. Moynihan, S.-K. Lee, M. Tatsumisago, and T. Minami. Estimation of activation energies for structural relaxation and viscous flow from DTA and DSC experiments. *Thermochim. Acta* **280/281**:153–162 (1996).
26. K. J. Crowley and G. Zografi. The use of thermal methods for predicting glass-former fragility. *Thermochim. Acta* **380**:79–93 (2001).
27. R. G. Strickley and B. D. Anderson. Solid-state stability of human insulin I. Mechanism and the effect of water on the kinetics of degradation in lyophiles from pH 2–5 solutions. *Pharm. Res.* **13**:1142–1153 (1996).
28. M. Karel and I. Saguy. Effects of water on diffusion in food systems. *Adv. Exp. Med. Biol.* **302**:157–173 (1991).
29. R. Bohmer, K. L. Ngai, C. A. Angell, and D. J. Plazek. Nonexponential relaxations in strong and fragile glass formers. *J. Chem. Phys.* **99**:4201–4209 (1993).
30. I. M. Hodge. Enthalpy relaxation and recovery in amorphous materials. *J. Non-Cryst. Solids* **169**:211–266 (1994).
31. F. Fujara, B. Geil, H. Sillescu, and G. Fleischer. Translational and rotational diffusion in supercooled orthoterphenyl close to the glass transition. *Z. Phys. B Condens. Matter* **88**:195–204 (1992).
32. A. J. D'Souza, R. L. Schowen, R. T. Borchardt, J. S. Salsbury, E. J. Munson, and E. M. Topp. Reaction of a peptide with polyvinylpyrrolidone in the solid state. *J. Pharm. Sci.* **92**:585–593 (2003).